# Sandwich-Stacked $SnO_2$/Cu Hybrid Nanosheets as Multichannel Anodes for Lithium Ion Batteries

**Junwen Deng,[†,‡,*] Chenglin Yan,[†,*] Lichun Yang,[†,▽] Stefan Baunack,[†] Steffen Oswald,[§] Horst Wendrock,[§] Yongfeng Mei,[⊥] and Oliver G. Schmidt[†,‡,∥,#]**

[†]Institute for Integrative Nanosciences, IFW Dresden, Helmholtzstraße 20, Dresden 01069, Germany, [‡]Material Systems for Nanoelectronics, Chemnitz University of Technology, Straße der Nationen 62, Chemnitz 09107, Germany, [§]Institute for Complex Materials, IFW Dresden, Helmholtzstraße 20, Dresden, 01069 Germany, [⊥]Department of Materials Science, Fudan University, Shanghai 200433, China, [∥]Center for Advancing Electronics Dresden, Dresden University of Technology, 01067 Dresden, Germany, and [#]Merge Technologies for Multifunctional Lightweight Structures, Chemnitz University of Technology, Straße der Nationen 62, Chemnitz 09107, Germany. [▽]Present address: School of Materials Science and Engineering, South China University of Technology, Guangzhou 510640, China.

**ABSTRACT** We have introduced a facile strategy to fabricate sandwich-stacked $SnO_2$/Cu hybrid nanosheets as multichannel anodes for lithium-ion batteries applying rolled-up nanotechnology with the use of carbon black as intersheet spacer. By employing a direct self-rolling and compressing approach, a much higher effective volume efficiency is achieved as compared to rolled-up hollow tubes. Benefiting from the nanogaps formed between each neighboring sheet, electron transport and ion diffusion are facilitated and $SnO_2$/Cu nanosheet overlapping is prevented. As a result, the sandwich-stacked $SnO_2$/Cu hybrid nanosheets exhibit a high reversible capacity of 764 mAh $g^{-1}$ at 100 mA $g^{-1}$ and a stable cycling performance of ~75% capacity retention at 200 mA $g^{-1}$ after 150 cycles, as well as a superior rate capability of ~470 mAh $g^{-1}$ at 1 A $g^{-1}$. This synthesis approach presents a promising route to design multichannel anodes for high performance Li-ion batteries.

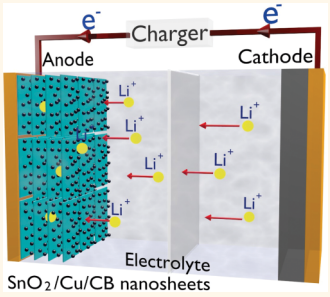


**KEYWORDS:** lithium-ion batteries · anodes · $SnO_2$ · stacked structures · two-dimensional nanosheets

Lithium-ion batteries (LIBs) have revolutionized portable electronics and become the dominant power sources for potential applications in electric vehicles (EV) and plug-in hybrid electric vehicles (HEV).[1−3] Further improvements in energy and power density put high demands on either new electrode materials or novel structure design.[4−6] As a potential substitute for commercially available graphite anodes (theoretical capacity 372 mAh $g^{-1}$), $SnO_2$ has a high theoretical capacity (781 mAh $g^{-1}$) and low potential of $Li^+$ intercalation.[7] Generally, $SnO_2$-based anodes suffer from poor electronic conductivity due to intrinsic nonstoichiometry arising from oxygen vacancies. In addition, large volume changes (~300%) during the lithiation/delithiation process inevitably generate mechanical strain, which leads to electrode disintegration and induces rapid capacity fading, making it a significant challenge to achieve superior electrochemical performance.[8] In order to improve the lithium storage capability for $SnO_2$-based electrodes, considerable efforts have been made toward tailoring material structures to enhance the electronic conductivity, accommodate volume changes and facilitate ion diffusion.[9]

Two-dimensional (2D) nanoarchitectures are particularly attractive for $Li^+$ storage owing to their unique structural properties and surface characteristics.[10] However, most 2D nanostructures have smooth facets, easily leading to tightly overlap and form agglomerates.[11] The tight overlapping of nanosheets reduces the active surface area and elongates ion diffusion paths, therefore, heavily hampering their application potential for energy storage. One promising solution to prevent such agglomeration is to create loosely stacked sandwich structures by employing additional additives such as nanotubes, ultrafine nanocarbons and graphene.[12−16] Recently, progress has been reported for $SnO_2$-graphene sandwich-like 2D architectures,[17−20] which

* Address correspondence to j.deng@ifw-dresden.de, c.yan@ifw-dresden.de.

Received for review April 30, 2013 and accepted July 23, 2013.

**Published online July 23, 2013**
**10.1021/nn402164q**

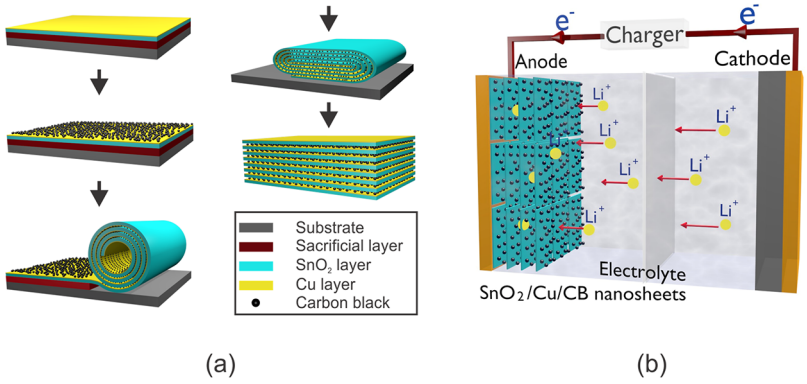


**Figure 1. (a) Schematic illustration of the roll-up and compression process of the stacked $SnO_2$/Cu hybrid nanosheets with carbon black (CB) uniformly dispersed between the layers; (b) schematic configuration of a stacked $SnO_2$/Cu cell with multichannel design using CB as the spacer, which provides lithium ion and electron "superhighways" for charge storage and delivery.**

exhibited superior electrochemical behaviors due to their fast ion diffusion and electron transport. In spite of that, most of these fabrication methods require complex processing, and the 2D framework of the structures is mainly limited to graphene nanosheets, upon which active materials are weakly anchored. Therefore, alternative facile and reliable synthetic routes are highly desirable to fabricate sandwich-like 2D nanostructures for high performance LIBs.

Rolled-up nanotechnology is a method employing strain engineering to change thin film in-plane dimensions. Because of stresses generated during film deposition, the stress (strain) gradient through the film thickness causes bending of the film upon release from the substrate. The thin film rolls up into a tubular structure if the film length is longer than one circumference along the rolling direction. This approach has been successfully employed to prepare strain-released microtubes for energy storage as reported previously.[21−25] The main drawback of the rolled-up tubes is the large hollow center, which limits their packing density and therefore the potential for further practical applications. In an attempt to increase the volume efficiency of self-wound nanomembranes, here, we apply rolled-up nanotechnology and a subsequent compression step to create compact sandwich-like nanosheet stacks. $SnO_2$/Cu bilayers are carefully strain engineered and, upon release from the substrate, automatically roll up into tubular structures with precoated carbon black (CB) periodically clamped between each winding. After compressing the rolled up microtubes with a pressure around 2.9 kPa, compact 2D nanosheet stacks with well-defined channels are readily created. With CB acting as the intersheet spacer, restacking and agglomeration of the $SnO_2$/Cu nanosheets are prevented during repeatable charge/discharge process, and volume changes can be accommodated by free channel space. In addition, these 2D nanosheets have large exposed surfaces for electrochemical reactions, from which ion kinetics as well as the interaction between active materials and the electrolyte is enhanced. Furthermore, the hybridized Cu thin layers not only function as a conductive layer to provide good electronic conductivity of the overall electrode, but also act as a structural buffer to preserve the integrity of the $SnO_2$ active layers. The multichannel anodes based on sandwich-stacked 2D $SnO_2$/Cu hybrid nanosheets thus exhibit a high reversible capacity of 764 mAh $g^{-1}$ at 0.1 A $g^{-1}$ and a stable cycling performance of ~75% capacity retention at 0.2 A $g^{-1}$ after 150 cycles, as well as superior rate capability.

## RESULTS AND DISCUSSION

The processing of sandwich-stacked $SnO_2$/Cu nanosheets with multiple channels is schematically illustrated in Figure 1a. A 50 nm-thick $SnO_2$ layer is first deposited on top of a precoated sacrificial layer (photoresist AR-P 3510), followed by deposition of a 3 nm-thick Cu layer by electron beam evaporation. Then, homogeneously dispersed CB/ethanol suspension is sprayed on the $SnO_2$/Cu bilayer films forming a cross-linked conductive framework. Metallic Cu, which does not react with the electrolyte and lithium ions during the electrochemical process, is employed to serve as the supporting layer because of its high stability and ideal conductivity. The physically deposited bilayers are hence uniformly contacted with strong affinity, and the structural integrity is well-maintained due to electrochemical inactivity of Cu. After drying at ambient conditions, the CB-coated $SnO_2$/Cu nanomembranes are released from the substrate by dissolving the sacrificial layer with acetone. Meanwhile, the $SnO_2$/Cu composite membranes together with CB automatically peel off from the substrate. As a result of the strain gradient induced by thermal expansion during deposition, the nanomembranes break up into micrometer-sized pieces because of strain pulling, during which these pieces roll up into tubular structures and clamp the

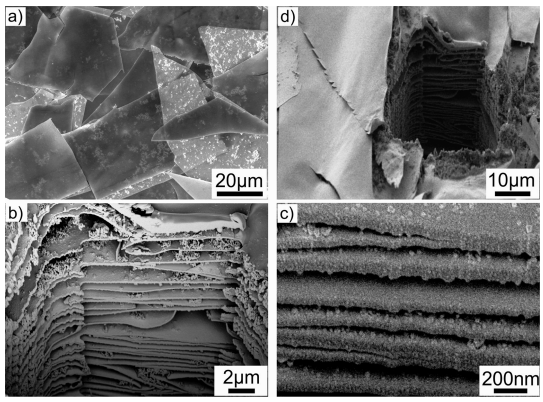


**Figure 2. (a) Top-view SEM image of the sandwich-stacked $SnO_2$/Cu nanosheets formed by rolled-up nanotech; (b−d) cross-sectional images of the electrodes composed of stacked $SnO_2$/Cu nanosheets with multichannel design using CB as the spacer. The CB maintains the electrical connectivity between the $SnO_2$/Cu nanosheets as a soft medium to buffer the stress of volume expansion and as a barrier against the reaggregation of $SnO_2$/Cu nanosheets during repeatable charge/discharge.**

CB framework in between the neighboring $SnO_2$/Cu windings (Figure S1). Under ~2.91 kPa external compression pressure, the tubular structures are subsequently flattened and partially slit at the edges[26] to form sandwich-stacked nanostructures (Figure S2). With CB embedded between alternating $SnO_2$/Cu hybrid nanosheets, these multichannel stacks are featured with enhanced mechanical property and effective utilization of interior space. Figure 1b shows schematic configuration of a cell model including stacked $SnO_2$/Cu nanosheets with CB spacer, which could establish lithium ion and electron "superhighways" for lithium ion delivery and storage.

The sample morphology was first characterized by scanning electron microscopy (SEM). Figure 2a shows a top-view SEM image of the as-prepared $SnO_2$/Cu sandwich-stacking, which reveals that the size of in-plane sheets is in the micrometer scale according to the pristine tube diameter ($\phi \sim 20\ \mu$m). The cross-sectional profile prepared by focus ion beam (FIB) cutting shows that CB as sandwich stuffing is tightly clamped between adjacent nanosheets (Figure 2b). The zoomed-in cross-sectional image in figure 2c displays smooth $SnO_2$/Cu hybrid layers with a total thickness of around 53 nm. A statistical study relating the CB cluster sizes to the heights of the multichannels is shown in Figure S3. The gaps, created by CB between adjacent layers, will not only provide open channels for $Li^+$ ion diffusion and electrolyte mass flow, but also offer free space for the volume expansion of $SnO_2$ during lithiation/delithiation processes, which opens up great opportunities to improve battery performance.

To further determine the element composition and uniformity, energy-dispersive X-ray (EDX) elemental mapping (Figure 3a) was carried out with a primary energy of 8 keV, which corresponds to a spatial resolution of about 300 nm. The sum spectrum confirms the composition of the as-prepared stacked $SnO_2$/Cu/CB nanosheets (Figure S4). The results suggest as-prepared samples are indeed composed of Sn, Cu and O elements as well as uniformly dispersed CB. X-ray photoelectron spectroscopy (XPS) analysis was performed to reveal the element stoichiometry of $SnO_2$. E-beam deposited $SnO_2$ was compared with a bulk $SnO_2$ reference sample. Figure 3b presents the Sn 3d core level binding energy spectra of the composite membranes at the surface, where two peaks at ~486.9 and ~495.0 eV, which are assigned to Sn $3d_{5/2}$ and $3d_{3/2}$, respectively, are detected.[27] At the sample surface, the Sn 3d spectra are in good agreement with the characteristic band of $SnO_2$, indicating that surface Sn is fully oxidized to $Sn^{4+}$. With 4 min presputtering ($Ar^+$, 3.5 keV), both Sn $3d_{5/2}$ and Sn $3d_{3/2}$ peaks are found to be slightly asymmetric, which indicates a nonstoichiometric oxygen deficiency ($SnO_{2-x}$) and a small amount of $Sn^{2+}$ existed in $SnO_2$ active layer. This is not found for the bulk reference sample and therefore not an effect resulting from ion beam damaging during sputtering. The phase structural of $SnO_2$/Cu was found to be amorphous, which was confirmed by X-ray Diffraction (XRD) (Figure S5).

To investigate the electrochemical behavior of the sandwich-stacked $SnO_2$/Cu hybrid nanosheets, control experiments are performed on pure $SnO_2$ nanosheets and $SnO_2$/Cu hybrid nanosheets, which are also prepared by self-rolling and further compressing. All the samples are tested at the same condition, with a current density of 100 mA $g^{-1}$ and a voltage cutoff in the range from 0.05 to 1.5 V. Figure 4a presents the first 10-cycle profiles of galvanostatic discharge/charge. It is clear that both cycling performance and Coulombic efficiency are improved when combining $SnO_2$ film with Cu thin layer (Figure S6), which attributes to the enhanced conductivity and structural stability.[28,29] The produced $Li_2O$ during lithation has been reported to be electrochemically inactive, which substantially decreases the Coulombic efficiency. But the incorporated ultrathin Cu can lead to partial electrochemical decomposition of $Li_2O$ particles during the charge process and improve the electrochemical performance of $SnO_2$ nanosheets.[30] Moreover, when CB is embedded into the hybrid nanosheets to create multichannels and prevent overlapping, a much better performance is achieved under the same measurement condition.

The detailed electrochemical processes concerning lithiation/delithiation of the sandwich-stacked $SnO_2$/Cu nanosheets were further investigated by cyclic voltammetry (CV). Figure 4b presents the CV curve at 0.1 mV/s scan rate in the potential window of 0−2 V. The reaction mechanism of $SnO_2$-based active materials is described by the following equations:[31]

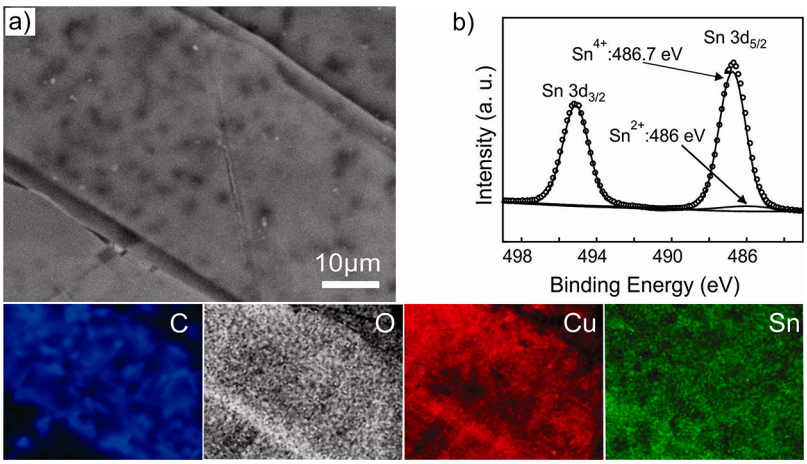


**Figure 3. (a) SEM image of the stacked $SnO_2$/Cu nanosheets and the corresponding C, O, Cu, Sn elemental mapping images using EDX at a primary energy of 8 keV; (b) XPS spectra of Sn $3d_{5/2}$ and Sn $3d_{3/2}$ for the stacked $SnO_2$/Cu nanosheets.**

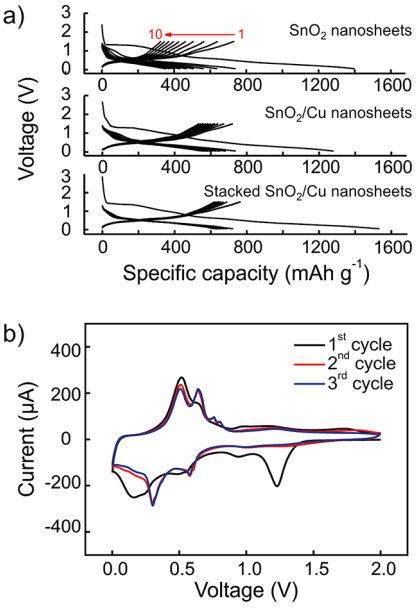


**Figure 4. (a) Charge−discharge voltage profiles for pure $SnO_2$ nanosheets, $SnO_2$/Cu nanosheets, and stacked $SnO_2$/Cu nanosheets cycled at a current density of 100 mA $g^{-1}$; (b) cyclic voltammogram of the stacked $SnO_2$/Cu nanosheets from 2 to 0 V *versus* Li/$Li^+$ at 0.1 mV/s scan rate; the first three cycles are shown.**

$$SnO_2 + 4Li^+ + 4e^- \rightarrow Sn + 2Li_2O \quad (1)$$

$$Sn + xLi^+ + xe^- \leftrightarrow Li_xSn \quad (0 \le x \le 4.4) \quad (2)$$

In the initial cycle, a broad reduction peak is observed at 1.25 V, which relates to eq 1 and describes the reduction of $SnO_2$ into element Sn and the formation of inactive $Li_2O$. The cathodic peak located around 0.9 V is attributed to the formation of a solid electrolyte interface (SEI) layer, which consumes $Li^+$ ions but can buffer and constrain the volume change thereafter. The two discussed peaks disappear in the following cycles, indicating the irreversibility of these two processes. In the reduction reaction, there are another two main peaks below 0.6 V, which are assigned to the alloying process of $Li_xSn$ shown in eq 2. During the reverse scanning, four anodic peaks in the voltage range of 0.4−0.9 V are observed, which relates to the $Li_xSn$ dealloying and $Li^+$ release process.[32] The coincidence of cycle 2 and cycle 3 indicates good repetition of the cycling performance, which is very consistent with the results of the galvanostatic discharge/charge curves shown in Figure 4a.

Figure 5a shows cycling performance of the sandwich-stacked $SnO_2$/Cu hybrid nanosheets as anode materials at a current density of 100 mA $g^{-1}$ for 100 cycles. The material delivers a high reversible capacity of 572 mA h $g^{-1}$ after 100 cycles, which retains 75% of its initial capacity. Such a stable cycling performance is superior to that of $SnO_2$ nanosheets and many other previously reported $SnO_2$-based nanostructures.[16] With higher current rates (500 and 1000 mA $g^{-1}$) applied, highly stable cycling performance is also obtained at each current density for 100 cycles. Similar to the electrode behavior at a current density of 100 mA $g^{-1}$, there is slight capacity decay over initial 10 cycles, which is plausibly explained by consumption of $Li^+$ for the formation of $Li_2O$ inactive phase and the SEI layer. Beyond the 10th cycle, the cycling stability becomes extremely good and the capacity retention remains at around 90% after 100 cycles.

In addition to the excellent cycling performance, these sandwich-like stacks also exhibit convincing rate capabilities. Figure 5b shows the rate capability of the anode, where a gradually increased current rate is applied to an assembled cell. Starting from 100 mA $g^{-1}$, a reversible capacity of 470 mAh $g^{-1}$ is obtained after 40 cycles at a current density as high as 1000 mA $g^{-1}$. When the discharge/charge current density is reduced back to 100 mA $g^{-1}$, the reversible capacity increases to 590 mAh $g^{-1}$ and stays above 580 mAh $g^{-1}$ in the following cycles. To evaluate the cycle life of the stacked $SnO_2$/Cu nanosheet electrodes, a current density of

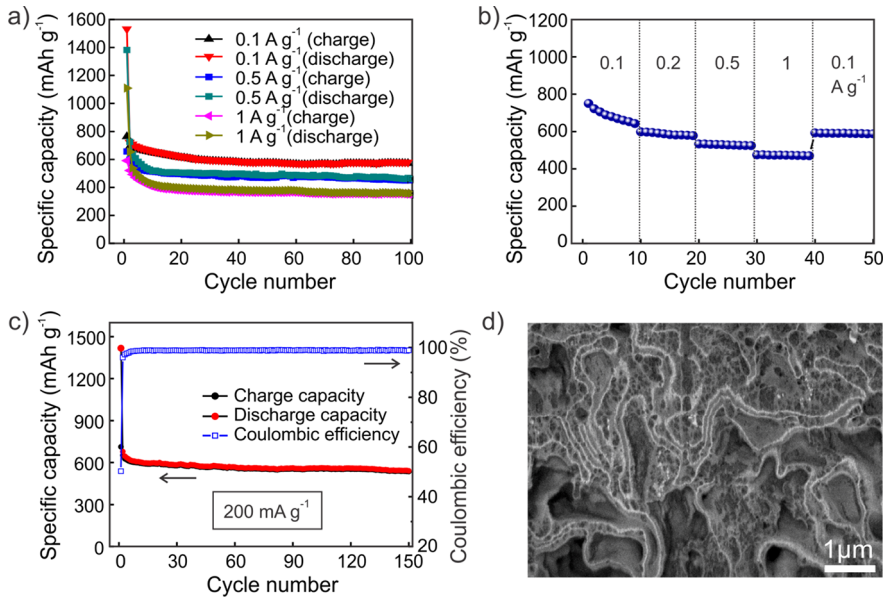


**Figure 5. Electrochemical characterization of the sandwich-stacked $SnO_2$/Cu nanosheets as anodes in lithium ion batteries: (a) comparative cycling performance showing the discharge and charge capacities of the sandwich-stacked $SnO_2$/Cu nanosheets at current rates of 100, 500, and 1000 mA $g^{-1}$; (b) rate capability of the stacked $SnO_2$/Cu nanosheets; (c) cycling performance for 150 cycles at a current rate of 200 mA $g^{-1}$ from 0.05 to 1.5 V *versus* $Li/Li^+$; (d) electron backscattering contrast on cross-sectional image of the stacked $SnO_2$/Cu nanosheets at a fully charged state after 100 cycles.**

200 mA $g^{-1}$ is applied for 150 cycles. As shown in Figure 5c, the first reversible capacity is 713 mAh $g^{-1}$, and a charge capacity of 535 mAh $g^{-1}$ can be retained after 150 cycles with capacity retention of 75%. The Coulombic efficiency is well above 98% from and subsequent to the second cycle.

The outstanding electrochemical performance is mainly ascribed to the new structure design of the $SnO_2$/Cu nanosheets. Using CB plays a key role in forming such sandwich-stacked structure. With CB as conductive intersheet spacer, restacking and agglomeration of $SnO_2$/Cu nanosheets are prevented, and the free channel space effectively accommodates volume changes during repeated charge/discharge processes; hence, stable cycling performance could be ensured by the structural stability. As the electrolyte seeps through the nanogaps between adjacent $SnO_2$/Cu nanosheets, there is an additional pathway created for $Li^+$ to reach the interior of the $SnO_2$/Cu nanosheets. Therefore, the sandwich-stacked $SnO_2$/Cu nanosheets help to enhance the rate capabilities of Li-ion batteries by providing higher electrode/electrolyte contact areas, increased number of Li-ion insertion sites, and reduced diffusion length in the intercalation $SnO_2$ nanosheets. Taking into account that the characteristic time constant $\tau$ for diffusion is proportional to the square of the diffusion length $L$ ($\tau \approx L^2/D$, where $L$ is the diffusion distance and $D$ is the coupled diffusion coefficient for $Li^+$ and $e^-$), the diffusion time $\tau$ for $Li^+$ will decrease by decreasing the diffusion length $L$, which finally leads to an excellent rate performance. In addition, the hybridization of Cu thin layer effectively enhances the electronic conductivity of the overall electrode, and the integrity of $SnO_2$ active layer is well preserved due to its structure restriction. Moreover, the nanosheets are formed by self-winding during film strain release. This could effectively ease the intrinsic strain and offer a minimization of the system energy, and thereby enhance the tolerance to stress cracking caused by lithiation/delithiation processes.

To further investigate the lithium-driven structural and morphological changes of the sandwich-stacked $SnO_2$/Cu nanosheet systems, we examined the cross-sectional profile of the stacked $SnO_2$/Cu nanosheets at the 100th fully charged state by FIB cutting. As depicted in Figure 5d, the stacked $SnO_2$/Cu nanostructures are still maintained and the whole structural integrity of the active electrode materials is preserved. The electron backscattering contrast in the image relates to different elements detected by the detector, and continuous white lines indicate the integrity of the $SnO_2$/Cu film. With repeated expansion and shrinking during lithation/delithation, the flat sheets twist and curl to form interconnected porous compounds because of the embedded CB, which in turn strengthens the stability of the electrode material. This is in accordance with the results in Figure 5c that there is no obvious capacity decay even after 150 cycles. Therefore, we conclude that the outstanding cycling performance relies on the distinctive stacked 2D nanosheet structures with its excellent structural stability.

## CONCLUSION

In summary, we employed compression of self-rolled nanostructures to fabricate novel sandwich-stacked two-dimensional nanosheets with CB uniformly

dispersed between each hybrid $SnO_2$/Cu nanosheet. The CB establishes the electrical connectivity between the $SnO_2$/Cu nanosheets as a soft medium to buffer the stress of volume expansion and acts as a barrier against the reaggregation of $SnO_2$/Cu nanosheets during repeatable charge/discharge. The multichannel design of the electrodes offers fast electron and ion transportation, leading to remarkably improved electrochemical performance. When probed as anode materials for lithium ion batteries in a half cell model, the sandwich-stacked $SnO_2$/Cu hybrid nanosheets exhibit significant improvement in cyclability compared to $SnO_2$ nanosheets and $SnO_2$/Cu hybrid nanosheets. A high capacity of 535 mAh $g^{-1}$ can be retained after 150 cycles at a current density of 200 mA $g^{-1}$ with 75% capacity retention. The proposed strategy is facile and general, which can be applied to the fabrication of other electrode materials with multichannel design, and enhanced electrochemical performance for lithium ion batteries should be expected.

## METHODS

**Sample Preparation.** A photoresist (ARP 3510, Allresist) as the sacrificial layer was first spin coated onto Si wafer substrates (3 in.) at 3500 rpm for 35 s prior to baking at 90 °C in an oven. A 50 nm $SnO_2$ film and a 3 nm Cu film were then deposited sequentially by electron beam evaporator (Edwards AUTO500). After sprinkling carbon black (CB) (Timcal) on the hybrid film (100 $\mu$L of 0.5 mg/mL CB-Ethanol suspension on each wafer), we thoroughly dried the CB-coated nanomembranes in air at room temperature. Then the samples were directly immersed into acetone to remove the sacrificial layer. In the process of photoresist dissolution, the composite membranes self-rolled into tubular structures clamping with CB. The tubes were then uniformly dispersed on a 3.0 in. Si wafer surface with a film thickness of roughly single tube height. By means of another Si wafer, 2.91 kPa pressure was applied to compress and flatten the tubes. During this process the edges of the tubes split to form sandwich-like 2D nanosheets.

**Material Characterization.** A FIB/SEM equipment (NVision 40 CrossBeam, Carl Zeiss) was used to investigate the morphology and cross-sectional profiles of the samples. The microstructure and chemical composition of the samples were investigated using a field-emission gun SEM scanning electron microscope (Zeiss Ultra 55 Plus, 8 keV) equipped with an energy-dispersive X-ray (EDX) spectroscopy instrument. The XPS measurements were carried out using a PHI 5600 CI (Physical Electronics) spectrometer. Raman analysis (from Renishaw) was performed with 442 nm wavelength to check the compositions.

**Electrochemical Characterization.** Swagelok cells were assembled in an Ar-filled glovebox ($H_2O$, $O_2$ < 0.1 ppm, Mbraun, Germany). Working electrodes were prepared by mixing the $SnO_2$/Cu nanosheets with conductive additive CB (Super P, Timcal) and polyvinylidene difluoride (PVDF, Aldrich) binder at a weight ratio of 70:20:10 in *N*-methyl-2-pyrrolidinone (NMP, Aldrich) solvent. The slurry was pasted onto a current collector (Cu foil, Goodfellow) and then dried in a vacuum oven at 80 °C for 10 h. The dried electrode was punched into $\phi = 10$ mm discs for cell assembly. Metallic Li foil (Aldrich) was used as both the counter and reference electrodes, and a glass fiber membrane (Whatman) was used as the separator. The electrolyte consisted of a solution of 1 M $LiPF_6$ in ethylene carbonate (EC)/dimethylcarbonate (DMC) (1:1, in wt %) obtained from Merck, including 2 vol % vinylene carbonate (VC) electrolyte additive (Merck). All the electrochemical tests are conducted on these cells, and the control samples are prepared at the same conditions. The cyclic voltammetry test was performed between 0 and 2 V *versus* $Li/Li^+$ at a scanning rate of 0.1 mV $s^{-1}$ *via* a Zahner electrochemical workstation (IM6ex). Galvanostatic cycling was carried out with an Arbin instrument BT2000 at a voltage rage of 0.05−1.5 V *versus* $Li/Li^+$ at different current densities. The pristine samples are composed of 90.9% $SnO_2$, 6.8% Cu, and 2.3% CB by weight; therefore, $SnO_2$ accounts for 64% of each electrode. The capacity in our work was calculated based on the total mass of the $SnO_2$/Cu nanosheets with CB.

*Conflict of Interest:* The authors declare no competing financial interest.

*Supporting Information Available:* SEM cross section image of the sandwich-stacked $SnO_2$/Cu nanosheets, statistical study of the CB cluster sizes, EDX spectrum and XRD pattern of the $SnO_2$/Cu nanosheets, and comparison study of cycling performance of the $SnO_2$-based nanosheet electrodes at a current density of 100 mA $g^{-1}$. This material is available free of charge *via* the Internet at http://pubs.acs.org.

*Acknowledgment.* This work was financed by the International Research Training Group (IRTG) project "Rolled-up nanotech for on-chip energy storage, G9" and PAKT project "Electrochemical energy storage in autonomous systems, Nr. 49004401".

## REFERENCES AND NOTES

1. Armand, M.; Tarascon, J. M. Building Better Batteries. *Nature* **2008**, *451*, 652–657.
2. Scrosati, B.; Garche, J. Lithium Batteries: Status, Prospects and Future. *J. Power Sources* **2010**, *195*, 2419–2430.
3. Thackeray, M. M.; Wolverton, C.; Isaacs, E. D. Electrical Energy Storage for Transportation—Approaching the Limits of, and Going beyond, Lithium-Ion Batteries. *Energy Environ. Sci.* **2012**, *5*, 7854–7863.
4. Arico, A. S.; Bruce, P.; Scrosati, B.; Tarascon, J.-M.; van Schalkwijk, W. Nanostructured Materials for Advanced Energy Conversion and Storage Devices. *Nat. Mater.* **2005**, *4*, 366–377.
5. Guo, Y.-G.; Hu, J.-S.; Wan, L.-J. Nanostructured Materials for Electrochemical Energy Conversion and Storage Devices. *Adv. Mater.* **2008**, *20*, 2878–2887.
6. Peter, G. B.; Bruno, S.; Jean-Marie, T. Nanomaterials for Rechargeable Lithium Batteries. *Angew. Chem., Int. Ed.* **2008**, *47*, 2930–2946.
7. Idota, Y.; Kubota, T.; Matsufuji, A.; Maekawa, Y.; Miyasaka, T. Tin-Based Amorphous Oxide: A High-Capacity Lithium-Ion-Storage Material. *Science* **1997**, *276*, 1395–1397.
8. Belliard, F.; Connor, P. A.; Irvine, J. T. S. Novel Tin Oxide-Based Anodes for Li-ion Batteries. *Solid State Ionics* **2000**, *135*, 163–167.
9. Chen, J. S.; Lou, X. W. $SnO_2$-Based Nanomaterials: Synthesis and Application in Lithium-Ion Batteries. *Small* **2013**, *9*, 1877–1893.
10. Yoo, E.; Kim, J.; Hosono, E.; Zhou, H.-s.; Kudo, T.; Honma, I. Large Reversible Li Storage of Graphene Nanosheet Families for Use in Rechargeable Lithium Ion Batteries. *Nano Lett.* **2008**, *8*, 2277–2282.
11. Liu, J.; Liu, X.-W. Two-Dimensional Nanoarchitectures for Lithium Storage. *Adv. Mater.* **2012**, *24*, 4097–4111.
12. Zheng, H. J.; Tang, F. Q.; Jia, Y.; Wang, L. Z.; Chen, Y. C.; Lim, M.; Zhang, L.; Lu, G. Q. Layer-By-Layer Assembly and Electrochemical Properties of Sandwiched Film of Manganese Oxide Nanosheet and Carbon Nanotube. *Carbon* **2009**, *47*, 1534–1542.
13. Wu, Z.-S.; Ren, W.; Wen, L.; Gao, L.; Zhao, J.; Chen, Z.; Zhou, G.; Li, F.; Cheng, H.-M. Graphene Anchored with $Co_3O_4$

Nanoparticles as Anode of Lithium Ion Batteries with Enhanced Reversible Capacity and Cyclic Performance. *ACS Nano* **2010**, *4*, 3187–3194.
14. Zhang, H. X.; Feng, C.; Zhai, Y. C.; Jiang, K. L.; Li, Q. Q.; Fan, S. S. Cross-Stacked Carbon Nanotube Sheets Uniformly Loaded with $SnO_2$ Nanoparticles: A Novel Binder-Free and High-Capacity Anode Material for Lithium-Ion Batteries. *Adv. Mater.* **2009**, *21*, 2299–2304.
15. Liu, J.; Chen, J. S.; Wei, X.; Lou, X. W.; Liu, X.-W. Sandwich-Like, Stacked Ultrathin Titanate Nanosheets for Ultrafast Lithium Storage. *Adv. Mater.* **2011**, *23*, 998–1002.
16. Ji, L.; Tan, Z.; Kuykendall, T.; An, E. J.; Fu, Y.; Battaglia, V.; Zhang, Y. Multilayer Nanoassembly of Sn-Nanopillar Arrays Sandwiched Between Graphene Layers for High-Capacity Lithium Storage. *Energy Environ. Sci.* **2011**, *4*, 3611–3616.
17. Wang, D.; Kou, R.; Choi, D.; Yang, Z.; Nie, Z.; Li, J.; Saraf, L. V.; Hu, D.; Zhang, J.; Graff, G. L.; *et al.* A. Ternary Self-Assembly of Ordered Metal Oxide−Graphene Nanocomposites for Electrochemical Energy Storage. *ACS Nano* **2010**, *4*, 1587–1595.
18. Su, Y.; Li, S.; Wu, D.; Zhang, F.; Liang, H.; Gao, P.; Cheng, C.; Feng, X. Two-Dimensional Carbon-Coated Graphene/Metal Oxide Hybrids for Enhanced Lithium Storage. *ACS Nano* **2012**, *6*, 8349–8356.
19. Wang, X.; Cao, X.; Bourgeois, L.; Guan, H.; Chen, S.; Zhong, Y.; Tang, D.-M.; Li, H.; Zhai, T.; Li, L.; *et al.* N-Doped Graphene-$SnO_2$ Sandwich Paper for High-Performance Lithium-Ion Batteries. *Adv. Funct. Mat.* **2012**, *22*, 2682–2690.
20. Ding, S.; Luan, D.; Boey, F. Y. C.; Chen, J. S.; Lou, X. W. $SnO_2$ Nanosheets Grown on Graphene Sheets with Enhanced Lithium Storage Properties. *Chem. Commun.* **2011**, *47*, 7155–7157.
21. Ji, H. X.; Wu, X. L.; Fan, L. Z.; Krien, C.; Fiering, I.; Guo, Y.-G.; Mei, Y.; Schmidt, O. G. Self-Wound Composite Nanomembranes as Electrode Materials for Lithium Ion Batteries. *Adv. Mater.* **2010**, *22*, 4591–4595.
22. Deng, J.; Ji, H.; Yan, C.; Zhang, J.; Si, W.; Baunack, S.; Oswald, S.; Mei, Y.; Schmidt, O. G. Naturally Rolled-Up C/Si/C Trilayer Nanomembranes as Stable Anodes for Lithium-Ion Batteries with Remarkable Cycling Performance. *Angew. Chem., Int. Ed.* **2013**, *125*, 2382–2386.
23. Yan, C. L.; Xi, W.; Si, W. P.; Deng, J. W.; Schmidt, O. G. Highly Conductive and Strain-Released Hybrid Multilayer Ge/Ti Nanomembranes with Enhanced Lithium-Ion-Storage Capability. *Adv. Mater.* **2013**, *25*, 539–544.
24. Schmidt, O. G.; Eberl, K. Nanotechnology: Thin Solid Films Roll Up Into Nanotubes. *Nature* **2001**, *410*, 168–168.
25. Mei, Y. F.; Huang, G.; Solovev, A. A.; Ureña, E. B.; Mönch, I.; Ding, F.; Reindl, T.; Fu, R. K. Y.; Chu, P. K.; Schmidt, O. G. Versatile Approach for Integrative and Functionalized Tubes by Strain Engineering of Nanomembranes on Polymers. *Adv. Mater.* **2008**, *20*, 4085–4090.
26. Zander, T.; Deneke, C.; Malachias, A.; Mickel, C.; Metzger, T.; Schmidt, O. G. Planar Hybrid Superlattices by Compression of Rolled-Up Nanomembranes. *Appl. Phys. Lett.* **2009**, *94*, 053102–053102−3.
27. Wang, C.; Du, G.; Ståhl, K.; Huang, H.; Zhong, Y.; Jiang, J. Ultrathin $SnO_2$ Nanosheets: Oriented Attachment Mechanism, Nonstoichiometric Defects, and Enhanced Lithium-Ion Battery Performances. *J. Phys. Chem. C* **2012**, *116*, 4000–4011.
28. Taberna, P. L.; Mitra, S.; Poizot, P.; Simon, P.; Tarascon, J. M. High Rate Capabilities $Fe_3O_4$-Based Cu Nano-Architectured Electrodes for Lithium-Ion Battery Applications. *Nat. Mater.* **2006**, *5*, 567–573.
29. Chen, H.; Xiao, Y.; Wang, L.; Yang, Y. Silicon Nanowires Coated With Copper Layer as Anode Materials for Lithium-Ion Batteries. *J. Power Sources* **2011**, *196*, 6657–6662.
30. Poizot, P.; Laruelle, S.; Grugeon, S.; Dupont, L.; Tarascon, J. M. Nano-Sized Transition-Metal Oxides as Negative-Electrode Materials for Lithium-Ion Batteries. *Nature* **2000**, *407*, 496–499.
31. Courtney, I. A.; Dahn, J. Electrochemical and *in Situ* X-Ray Diffraction Studies of the Reaction of Lithium with Tin Oxide Composites. *J. Electrochem. Soc.* **1997**, *144*, 2045–2052.
32. Brousse, T.; Retoux, R.; Herterich, U.; Schleich, D. Thin-Film Crystalline $SnO_2$-Lithium Electrodes. *J. Electrochem. Soc.* **1998**, *145*, 1–4.